Journal of Microbiology, Immunology and Infection 57 (2024) 128—137

Available online at www.sciencedirect.com

ScienceDirect

journal homepage: www.e-jmii.com

Original Article

Genomic epidemiology of hypervirulent carbapenem-resistant *Klebsiella pneumoniae* at Jinshan local hospital, Shanghai, during 2014—2018

Ming-Quan Guo [a], Yi-Ting Wang [b], Shan-Shan Wang [c], Li-Kuang Chen [a,d], Ying-Hua Xu [c,*], Gang Li [b,]**

[a] *Department of Laboratory Medicine, Shanghai Public Health Clinical Center, Fudan University, Shanghai, 200025, China*
[b] *Department of Laboratory Medicine, Jinshan Hospital, Shanghai Medical College, Fudan University, Shanghai, China*
[c] *Key Laboratory of the Ministry of Health for Research on Quality and Standardization of Biotech Products, National Institutes for Food and Drug Control, Beijing, 102629, China*
[d] *Department of Laboratory Medicine, Clinical Pathology, Buddhist Tzu Chi General Hospital, Hualien, Taiwan*

Received 22 March 2023; received in revised form 23 September 2023; accepted 29 October 2023
Available online 2 November 2023

KEYWORDS
Hypervirulent carbapenem-resistant *Klebsiella pneumoniae*;
Genomic epidemiology;
Virulence plasmid;
Carbapenem resistance gene

Abstract *Background:* Hypervirulent carbapenem-resistant *Klebsiella pneumoniae* (Hv-CRKP) triggered a significant public health challenge. This study explored the prevalence trends and key genetic characteristics of Hv-CRKP in one Shanghai suburbs hospital during 2014—2018.
Methods: During five years, Hv-CRKP strains identified from 2579 CRKP by specific PCR, were subjected to performed short- and long-read sequencing technology; epidemiological characteristics, antimicrobial-resistance genes (ARGs), virulence determinants, detailed plasmid profiles and conjugation efficiency were comprehensively investigated.
Results: 155 Hv-CRKP and 31 non-Hv-CRKP strains were sequenced. Hv-CRKP strains exhibited significant resistance to six common antibiotic classes (>92%). ST11 steadily increased and became the most prevalent ST (85.2%), followed by ST15 (8.5%), ST65 (2.6%), ST23 (1.9%), and ST86 (0.6%). ST11-KL64 (65.2%) rapidly increased from 0 in 2014 to 93.9% in 2018. bla_{KPC-2} was the primary carbapenemase gene (97.4%). Other ARGs switched from *aac(3)-IId* to *aadA2* in aminoglycoside and from *sul1* to *sul2* in sulfanilamide. The time-dated phylogenetic tree was divided into four independent evolutionary clades. Clade 1 and 3 strains were mostly limited in the ICU, whereas Clade 2 strains were distributed among multiple departments. Compared to *ybt14* in

* Corresponding author.
** Corresponding author.
E-mail addresses: xuyh@nifdc.org.cn (Y.-H. Xu), li_gang@fudan.edu.cn (G. Li).

https://doi.org/10.1016/j.jmii.2023.10.012

ICEKp12 in Clade 1, Clade 3 strains harbored *ybt9* in ICEKp3 and $bla_{CTX-M-65}$. Hv-CRKP infected more wards than non-Hv-CRKP and showed greater transmission capacity. Three plasmids containing crucial carbapenemase genes demonstrated their early transmission across China.
Conclusion: The Hv-CRKP ST11-KL64 has rapidly replaced ST11-KL47 and emerged as the predominant epidemic subtype in various hospital wards, highlighting the importance of conducting comprehensive early surveillance for Hv-CRKP, especially in respiratory infections.

Introduction

Klebsiella pneumoniae, as an opportunistic pathogen, can cause a variety of hospital-acquired infections (HAI), especially in the elderly and immunocompromised individuals.[1] This organism accounts for about a third of all Gram-negative infections worldwide.[2] Compared to classical *K. pneumoniae* (cKp), hypervirulent *K. pneumoniae* (hvKp) typically causes life-threatening community-acquired infections (CAI), including liver abscesses and other invasive syndromes.[3] This hypervirulent phenotype of hvKP was believed to be caused by the presence of a virulence plasmid including two capsular polysaccharides (CPS) regulator genes (*rmp*A and *rmp*A2) and several siderophore gene clusters (such as *iuc*, *iro*, etc.).[4] Besides hvKP, another worrying development is the evolution of carbapenem-resistant *K. pneumoniae* (CRKP), associated with severe morbidity and death in global public health.[5] One of the most critical resistance mechanisms in CRKP is the production of carbapenemases, including bla_{KPC}, bla_{NDM} and bla_{OXA-48} family. Since the initial report of CRKP appearance in China in 2007,[6] it has been progressively isolated in clinical settings. The Chinese Antimicrobial Surveillance Network (www.chinets.com/) stated that the resistance rates of *K. pneumoniae* to meropenem in China increased dramatically from 2.9% in 2007 to 24.4% in 2021.

However, reports on the convergence of CRKP and hvKP strains are gradually increasing.[7] Since then, this convergence of carbapenem-resistant and hypervirulent strains has been detected all across the globe, with China being one of the most endemic countries.[8] Hv-CRKP, possessing high transmissibility, high resistance, and hypervirulence, is regarded as the superbug of the next generation.[9]

This study investigated the epidemiological characteristics, drug resistance profiles, and critical virulence determinants of the Hv-CRKP strains in a Shanghai local hospital from 2014 to 2018. Our findings will provide new insights into the hybrid evolutionary mechanisms of key virulence genes and ARGs, comprehensive plasmid profiles, and targeted early warning for Hv-CRKP strains.

Methods

Bacterial strains and identification

Between September 2014 and August 2018, we collected 2579 unique CRKP clinical isolates from diverse clinical specimens in one Jinshan hospital, Shanghai. All strains were cultured on Columbia blood agar plate and identified using the VITEK 2 system (bioMérieux, Marcy l'Etoile, France). Antibiotic Susceptibility results were screened using the Kirby—Bauer disc diffusion test. This study characterized CRKP isolates resistant to imipenem or meropenem (zone diameter $\leq$19 mm) according to CLSI and EUCAST guidelines.[10] Then, the Hv-CRKP isolates were identified from CRKP isolates using a two-step process.[11] PCR was initially used to identify virulence genes, specifically *rmp*A and/or *rmp*A2. Then, the positive strains with *rmp*A or *rmp*A2 were validated using the string test (viscous string $>$ five mm). All clinical information was obtained from the hospital's clinical charting systems. The Ethics Committee of Jinshan Hospital authorized this investigation.

Antimicrobial susceptibility testing

The Kirby—Bauer disc diffusion assay (K—B) was utilized to determine antimicrobial susceptibility, with results interpreted according to CLSI[10] and EUCAST breakpoints.[12] Tested antibiotics included amikacin, gentamicin, cefazolin, cefuroxime, cefotaxime, ceftazidime, cefepime, ciprofloxacin, imipenem, meropenem, tigecycline, colistin, ceftolozane-tazobactam (Thermo Fisher Scientific, Waltham, MA, USA). *Escherichia coli* ATCC 25922 was employed as a quality-control isolate.

Whole-genome sequencing and bioinformatic analysis

According to the criteria of one strain and one patient every 3 months for each department, 155 from 560 confirmed Hv-CRKP strains, and 31 non-Hv-CRKP strains during the same period were included for whole-genome sequencing (Table S1 and Table S2). Raw data were trimmed and filtered using fastp[13] to produce high-quality data. Then the genome data were assembled using SPAdes 3.14.1.[14] Genomic sequences were annotated with Prokka 1.14.6.[15]

Sequence types (STs), ARGs, virulence-associated genes, resistance score, virulence score, and capsule serotype (K) and O antigen (LPS) serotype prediction were identified using Kleborate 2.1.0.[16] A core single nucleotide polymorphisms (SNP)-based tree was established by PGCGAP 1.0.35.[17] An inferred timed phylogenetic tree was built by

BactDating 1.1 with default parameter,[18] using the core SNP tree and isolation dates of strains as the input files.

As of September 2022, we queried the NCBI database for the complete *K. pneumoniae* genomes identified in China. Then, according to the virulence score $\geq$3 and resistance score $\geq$2, predicted by Kleborate, we downloaded 135 reference Hv-CRKP complete genomes (Table S3). Then, this study included 155 Hv-CRKP strains and 135 Chinese reference Hv-CRKP strains for comparative genome analysis. A maximum likelihood (ML) phylogenetic tree was generated by FastTree 2.1.10.[19] The ML tree was visualized and annotated by the online tool iTOL v5.[20]

Three isolates (SH352, SH500, and SH552) from different phylogenetic clades were further subjected to long-read genome sequencing using the PacBio RS II system (Personalbio, Shanghai, China). Plasmid replicon types were identified by PlasmidFinder 2.1.6.[21] ARGs were identified by ResFinder.[22] Comparative analysis of plasmid sequences and specific genetic environments surrounding the carbapenemase-resistant genes was performed using BLAST, and the results were visualized with Easyfig2.2.5.[23] The presence of plasmids was analyzed based on the BLAST results.

Plasmid conjugation experiments

Donor isolates of plasmid conjugation assay were SH352, SH500, and SH552. The recipient strain was rifampicin-resistant *E.coli* C600. Briefly, Each of the three donor isolates and recipient strain C600 were co-cultured in LB broth until the logarithmic growth phase before being mixed at a ratio of 1:3[24] Transconjugants were selected on LB agar plates containing rifampicin (300 μg/mL) and meropenem (2 μg/mL). The conjugation frequency was calculated with three parallel replicates.

Galleria mellonella infection

We used the *G. mellonella* infection model to assess the *in vitro* virulence and lethality of *K. pneumoniae* strains.[8] Six strains with different virulence scores were evaluated their various virulence (SH416, 0; SH352, 1; SH419, 3; SH503, 4; SH552, 4; SH509, 5). PBS and *K. pneumoniae* NTUH-K2044 (high-virulence strain) were the negative and positive controls, respectively. The bacterial suspension was cultured into 1×10^8 CFU/mL. A 25-μL microsyringe was used to inject 10 μL of bacterial suspension into each larvae. After injection, larvae were incubated in plates at 37 °C for 3 days. Each group contained 10 larvae, and the experiment was repeated three times.

Statistical analysis

All data were analyzed using GraphPad Prism 9.0. $P < 0.05$ was considered as statistical significance.

Data availability

The whole genome sequences in this study have been deposited in the Genome Warehouse in the National Genomics Data Center, China National Center for Bioinformation,[25,26] with Bioproject Accession: PRJCA012185.

Results

Critical clinical characteristics of the Hv-CRKP patients

Between 2014.09 and 2018.08, our study comprised 2579 patients with culture-positive results for CRKP from Jinshan Hospital. A total of 560 Hv-CRKP isolates (21.7%) were discovered using a positive PCR results with the *rmp*A and (or) *rmp*A2 gene (Fig.S1). There was the highest prevalence of Hv-CRKP (269/769, 35.0%) in 2017, followed by 2016 (194/559, 34.7%), 2015 (46/473, 9.7%), 2018 (39/351, 11.1%), and 2014 (12/427, 2.8%). Throughout these years, the prevalence of Hv-CRKP in CRKP has steadily increased compared to 2014 ($P < 0.001$).

The clinical features of 560 individuals infected with Hv-CRKP strains were conducted (Table 1). The median age was sixty, while the maximum period was ninety-seven. The number of male patients (398/560, 71.1%) is substantially more significant than the proportion of female patients (28.9%) ($P = 0.002$). These strains were obtained from various source collections, including 347 (62.0%) from sputum, 90 (16.0%) from urine, 48 (8.6%) from blood, and 75 (13.4%) from other sources. As shown in Table 1, the intensive care unit (ICU) found the most Hv-CRKP isolates (333, 59.5%), followed by the departments of gastroenterology (45, 8.0%), infectious diseases (41, 7.3%), and neurosurgery (31, 5.5%). The detection rate of Hv-CRKP in the ICU was greater than that in other wards ($P < 0.001$).

All Hv-CRKP strains exhibited substantial carbapenem resistance (Table 1), especially to meropenem (98.9%) and imipenem (98.0%). In addition, these isolates revealed high level of resistance to aminoglycosides (92.0%), fluoroquinolones (98.4%), nitrofuran (99.6%), cephalosporins (1st and 2nd generation) (99.5%), and cephalosporins (3rd, 4th, and 5th generation) (99.8%). All of these strains were susceptible to tigecycline.

Molecular characteristics of the 155 Hv-CRKP strains

Among the 155 Hv-CRKP strains, ST11 was the most prevalent ST (132/155, 85.2%), followed by ST15 (8.5%), ST65 (2.6%), ST23 (1.9%), ST86, ST1049, and ST2357 (0.6%, each) (Table 2). And the percentage of ST11 detection increased steadily from 40% in 2014 to 93.9% in 2018. In contrast, the detection rate of the remaining STs was relatively low. K—O serotyping results were KL64-O1/O2v1 (101, 65.2%), followed by KL47-OL101 (18, 11.6%) and KL24-O1/O2v1 (8, 5.2%). KL64 and KL47 accounted for 101 (65.2%) and 26 (16.8%). In addition, the detection rate of KL64 climbed annually from 0 in 2014 to 93.9% in 2018, whereas the detection rate of KL47 has declined from 30% in 2014 to 0 in 2018 (Table 2). Three O surface antigens were observed. The detection rate of O1/O2v1 remained

Table 1 Clinical characteristics and antimicrobial resistance of 560 hv-CRKP strains.

Wards		ICU	Gastroenterology	Infectious Diseases	Neurosurgery	Geriatrics	Outpatient	Others	Total	*P Value*
Age, median, IQR		60 (47,69)	53 (45,61)	67 (52,75)	60 (43,68)	91 (89,95)	62 (58,73)	55 (47,68)	60 (48,70)	<0.001
Sex										
	Male	243 (73.0%)	37 (82.2%)	21 (51.2%)	19 (61.3%)	21 (84.0%)	8 (44.4%)	49 (73.1%)	398 (71.1%)	0.002
	Female	90 (27.0%)	8 (17.8%)	20 (48.8%)	12 (38.7%)	4 (16.0%)	10 (55.6%)	18 (26.9%)	162 (28.9%)	
Specimen Type										
	Sputum	239 (71.8%)	8 (17.8%)	14 (34.1%)	28 (90.3%)	14 (56.0%)	8 (44.4%)	36 (53.8%)	347 (62.0%)	<0.001
	Urine	43 (12.9%)	2 (4.4%)	13 (31.7%)	2 (6.5%)	10 (40.0%)	9 (50.0%)	11 (16.4%)	90 (16.0%)	
	Blood	23 (6.9%)	6 (13.4%)	9 (22.0%)	0	0	0	10 (14.9%)	48 (8.6%)	
	Others	28 (8.4%)	29 (64.4%)	5 (12.2%)	1 (3.2%)	1 (4.0%)	1 (5.6%)	10 (14.9%)	75 (13.4%)	
Year										
	2014	9 (2.7%)	0	0	0	1 (4.0%)	0	2 (3.0%)	12 (2.1%)	<0.001
	2015	25 (7.6%)	2 (4.4%)	5 (12.2%)	4 (12.9%)	2 (8.0%)	1 (5.6%)	7 (10.4%)	46 (8.3%)	
	2016	119 (35.7%)	15 (33.3%)	0	10 (32.3%)	17 (68.0%)	3 (16.6%)	30 (44.8%)	194 (34.6%)	
	2017	146 (43.8%)	28 (62.3%)	36 (87.8%)	15 (48.3%)	5 (20.0%)	14 (77.8%)	25 (37.3%)	269 (48.0%)	
	2018	34 (10.2%)	0	0	2 (6.5%)	0	0	3 (4.5%)	39 (7.0%)	
Antimicrobial resistance										
	Aminoglycosides	312 (93.7%)	41 (91.1%)	41 (100.0%)	23 (74.2%)	24 (96.0%)	18 (100.0%)	56 (83.6%)	515 (92.0%)	<0.001
	Fluoroquinolones	330 (99.1%)	44 (97.8%)	41 (100.0%)	28 (90.3%)	25 (100.0%)	18 (100.0%)	65 (97.0%)	551 (98.4%)	0.013
	Nitrofuran	332 (99.7%)	45 (100.0%)	40 (97.6%)	31 (100.0%)	25 (100.0%)	18 (100.0%)	67 (100.0%)	558 (99.6%)	0.459
	Cephalosporins (1st and 2nd generation)	330 (99.1%)	45 (100.0%)	41 (100.0%)	31 (100.0%)	25 (100.0%)	18 (100.0%)	67 (100.0%)	557 (99.5%)	0.914
	Cephalosporins (3rd, 4th, and 5th generation)	332 (99.7%)	45 (100.0%)	41 (100.0%)	31 (100.0%)	25 (100.0%)	18 (100.0%)	67 (100.0%)	559 (99.8%)	0.995
	Carbapenems	332 (99.7%)	45 (100.0%)	41 (100.0%)	30 (96.8%)	25 (100.0%)	18 (100.0%)	66 (98.5%)	557 (99.5%)	0.38
	Tigecycline	0	0	0	0	0	0	0	0	–
	Polymyxins	0	0	0	0	0	0	2 (3.0%)	2 (0.4%)	0.022
Total		333 (59.5%)	45 (8.0%)	41 (7.3%)	31 (5.5%)	25 (4.5%)	18 (3.2%)	67 (12.0%)	560	<0.001

high, whereas the detection rate of OL101 eventually fell to zero (Table 2).

The vast majority of 155 Hv-CRKP isolates harbored the bla_{KPC-2} carbapenemase gene (151, 97.4%), followed by $bla_{OXA-232}$ (1.3%), bla_{KPC-3} (0.6%), and bla_{NDM-5} (0.6%) (Table 2). All ST11 strains only carried bla_{KPC-2}. These bacteria also possessed a high rate of extended-spectrum-beta-lactamase (ESBL) gene (136, 87.7%). bla_{CTX-M} genes were detected in 85.8% of Hv-CRKP isolates, with $bla_{CTX-M-65}$ being the major bla_{CTX-M} gene (Table 2). The detection rate of strains carried by both $bla_{CTX-M-65}$ and bla_{SHV-12} grew dramatically from 20% in 2014 to 69.7% in 2018. Besides, we also observed a high prevalence of porin defects in these strains, such as truncation or loss in OmpK35 (134/155, 86.5%) and OmpK36GD mutation (132/155, 85.2%). Mutations in OmpK35 ($P < 0.001$) and OmpK36GD ($P = 0.012$) showed significant statistical differences in the distribution between the Hv-CRKP group and the non-Hv-CRKP group.

aadA2 (65.8%) and *aac* (3)-*IId* (18.1%) were the two primary aminoglycoside resistance genes. The rate of *aadA2* was from 20% in 2014 to 90.9% in 2018. In addition, the *qnrS1* gene associated with quinolone resistance was discovered in 63.2% of isolates, and its detection rate increased from 40% in 2014 to 93% in 2018. We found sulfonamide resistance mediated by *sul1* (11.6%) and *sul2* (61.3%). *sul2* was discovered more often over time, whereas *sul1* was detected less frequently.

Among these Hv-CRKP genomes, the predominance of siderophores was *iuc* 100%, *ybt* 99.4%, *iro* 12.3%, *and clb* 5.2%. The frequency of the *rmp*ADC was 70.3%. The

Table 2 Molecular characteristics of 155 hv-CRKP strains during 2014–2018.

Year	2014 (n = 10)	2015 (n = 11)	2016 (n = 41)	2017 (n = 60)	2018 (n = 33)	Total (n = 155)	*P value*
Sequence type							
ST11	4 (40.0%)	9 (81.8%)	36 (87.8%)	52 (86.6%)	31 (93.9%)	132 (85.2%)	<0.001
ST15	5 (50.0%)	2 (18.2%)	0	6 (10.0%)	0	13 (8.5%)	
ST23	0	0	1 (2.4%)	0	2 (6.1%)	3 (1.9%)	
ST65	0	0	4 (9.8%)	0	0	4 (2.6%)	
ST86	0	0	0	1 (1.7%)	0	1 (0.6%)	
ST2357	1 (10.0%)	0	0	0	0	1 (0.6%)	
ST1049	0	0	0	1 (1.7%)	0	1 (0.6%)	
K loci							
KL64	0	2 (18.2%)	22 (53.7%)	46 (76.7%)	31 (93.9%)	101 (65.2%)	<0.001
KL47	3 (30.0%)	7 (63.6%)	12 (29.3%)	4 (6.7%)	0	26 (16.8%)	
KL24	4 (40.0%)	2 (18.2%)	0	2 (3.3%)	0	8 (5.2%)	
Others	1 (10.0%)	0	7 (17.0%)	6 (10.0%)	2 (6.1%)	24 (12.9%)	
Unknown	2 (20.0%)	0	0	2 (3.3%)	0	4 (2.6%)	
O locus							
O1/O2v1	6 (60.0%)	4 (36.4%)	24 (58.6%)	55 (91.7%)	31 (93.9%)	119 (76.8%)	<0.001
OL101	4 (40.0%)	7 (63.6%)	5 (12.2%)	3 (5.0%)	0	19 (12.3%)	
O1/O2v2	0	0	5 (12.2%)	2 (3.3%)	2 (6.1%)	9 (5.8%)	
Unknown	0	0	7 (17.0%)	1 (1.7%)	0	8 (5.1%)	
Carbapenemases							
blaKPC-2	10 (100.0%)	11 (100.0%)	40 (97.6%)	57 (95.0%)	33 (100.0%)	151 (97.4%)	0.815
blaNDM-5	0	0	1 (3.6%)	0	0	1 (0.6%)	
blaKPC-3	0	0	0	1 (1.7%)	0	1 (0.6%)	
blaOXA-232	0	0	0	2 (3.3%)	0	2 (1.3%)	
ESBL							
blaCTX-M-65	2 (20.0%)	7 (63.6%)	24 (58.5%)	34 (56.7%)	6 (18.2%)	73 (47.1%)	<0.001
blaSHV-12	0	0	0	2 (3.3%)	1 (3.0%)	3 (1.9%)	
blaCTX-M-65 +*SHV-12*	2 (20.0%)	2 (18.2%)	12 (29.3%)	14 (23.3%)	23 (69.7%)	53 (34.2%)	
Others	2 (10.0%)	0	1 (2.4%)	4 (6.7%)	0	7 (4.5%)	
Negative	4 (40.0%)	2 (18.2%)	4 (9.8%)	6 (10.0%)	3 (9.1%)	19 (12.3%)	
Virulence genes							
Yersiniabactin	9 (90.0%)	11 (100.0%)	41 (100.0%)	60 (100.0%)	33 (100.0%)	154 (99.4%)	0.006
Colibactin	1 (10.0%)	0	5 (12.2%)	0	2 (6.1%)	8 (5.2%)	0.074
Aerobactin	10 (100.0%)	11 (100.0%)	41 (100.0%)	60 (100.0%)	33 (100.0%)	155 (100.0%)	–
Salmochelin	3 (30.0%)	4 (36.4%)	6 (14.6%)	4 (6.7%)	2 (6.1%)	19 (12.3%)	0.013
rmpADC	3 (30.0%)	6 (54.5%)	30 (73.2%)	28 (46.7%)	33 (100.0%)	109 (70.3%)	<0.001
rmpA2	10 (100.0%)	10 (90.9%)	41 (100.0%)	59 (98.3%)	33 (100.0%)	153 (98.7%)	0.17

prevalence of *rmp*ADC has increased significantly during the previous five years ($P < 0.001$). Moreover, the *rmp*A2 gene was found in 98.7% of strains.

Time-dated phylogeny of 186 clinical *K. pneumoniae* isolates

Time-dated phylogenetic analyses resolved these strains into four primary clades 1–4, with subclades 3.1–3.4 distinguishable within the largest clade 3 (Fig. 1). The Clade 1 comprised 21 strains, 16 in the Clade 2, 145 in the Clade 3, and 4 in the Clade 4. The Clade 1 strains were primary ST15 clones, The Clade 2 comprised diverse ST clones, The Clade 3 were ST11 clones, and the Clade 4 were ST23 clones. This tree indicated that the Clade 1 strains shared a most recent common ancestor in 1981, the Clade 2 in 1978, the Clade 3 in 1995, and the Clade 4 in 2015.

Strains within the Clades 1 and 3 were restricted in ICU from 2014 to 2018. Isolates of the Clade 4 were primarily recovered from ICU in 2018, whereas the Clade 2 was obtained from several departments between 2014 and 2018. All isolated in 2018 were concentrated in Clade 3.2, the largest sub-clade of the Clade 3. The Clade 3.1 strains were only found in 2017. Both of the Clade 3.3 and 3.4 strains were primarily recovered in 2016 and 2017. Importantly, non-Hv-CRKP strains were not found in outpatient and infection disease departments compared to Hv-CRKP.

There was a significant difference in the distribution of yersiniabactin in clades 1 and 3. *ybt9* in ICEKp3 was predominantly found in clade 3 (143/145, 98.6%), whereas *ybt14* in ICEKp12 was only found in clade 1 (19/21, 90.5%). Clade 3 strains were deeply related to *fosA3* and $bla_{\text{CTX-M-65}}$. In clade 3, most non-Hv-CRKP strains were in clade 3.3 (11/13, 84.6%). *clb2* and *clb3* were substantially associated with the Clade 4 and Clade 2, respectively. The distribution of resistance genes in clade 4 was significantly lower than in other clades ($P < 0.001$).

Comparative genome analysis

The phylogenetic tree was composed of three major clades (Fig. 2). Clade 1 and Clade 3 consisted primarily of ST11 clones, with 100% (108/108) and 97.8% (137/140), respectively. Over half of the Clade 1 strains were isolated in 2017, while most clade 3 strains were isolated in 2018. Most of the Clade 1 reference strains were isolated in Shanghai, while most Clade 3 reference strains were obtained in Zhejiang. This may suggest that the Clade 1 Hv-CRKP isolates were restricted to Shanghai, but the Clade 3 Hv-CRKP isolates were distributed throughout Shanghai and Zhejiang. The Clade 2 possessed numerous hypervirulent STs, including ST15, ST23, ST65, and ST86. The Clade 3 predominantly carried KL64 (79/140, 56.4%) and KL47 (50/140, 35.7%), whereas the Clade 1 had KL64. the Clade 2 possessed more varied carbapenemase than the other two clades (mainly carrying $bla_{\text{KPC-2}}$). $bla_{\text{OXA-232}}$ were discovered in the Clade 2 but were absent from all different clades. $bla_{\text{CTX-M-65+SHV-12}}$ was detected primarily in Clades 1 and 3, while $bla_{\text{CTX-M-15}}$ was predominant in clade 2. The *fosA3* gene was mainly detected in Clades 1 and 3. Regarding the *ybt* virulence gene, the Clade 1 predominantly carried *ybt14*-ICEKp12 and *ybt1*-ICEKp10, whereas the other two clades essentially had *ybt9*-ICEKp3.

Important characteristics of virulence and resistance plasmids

According to the combined short- and long-read sequencing results, strain SH352, SH500, and SH552 have respective genome sizes of 6,290,840, 6,175,253, and 5,983,274bp. These three genomes had one chromosome and seven plasmids (Fig. 3). A plasmid carrying *rmp*A2 was identified (pSH552p1, 256,515 bp). Two $bla_{\text{KPC-2}}$ carrying plasmids (pSH500p2, 170,835 bp and pSH552p3, 106,850 bp) and one $bla_{\text{NDM-1}}$ carrying plasmid (pSH352p3, 112,642 bp) were found. Both pSH352p3 and pSH500p2 were IncFII plasmids. Unlike most 170 kb KPC-2-encoding plasmids, pSH552p2 belonged to the cointegrated FII (pBK30683) plasmid.[27] In Fig. 3B, pSH500p2 was transmitted to numerous wards, such as the ICU, the Department of Infectious Diseases, and Gastroenterology. And the dissemination of the pSH552p2 was restricted to the ICU, Neurosurgery, and Geriatrics.

The structure surrounding $bla_{\text{NDM-1}}$ was *rmtC-*$bla_{\text{NDM-1}}$*-ble-trpF-dsbD-cutA-groS-groL-IS3*. The genomic environments surrounding $bla_{\text{KPC-2}}$ indicated the presence of two distinct genetic structures. The structure of surrounding $bla_{\text{KPC-2}}$ of pSH500p2 was *IS26-ISKpn6-*$bla_{\text{KPC-2}}$*-ISKpn27-Tn3-IS26*, while pSH552p2 was *IS26-Tn3-hin-klcA-*$bla_{\text{KPC-2}}$*-ISKpn27-Tn3-IS26*. Both types were composite transposons based on *IS26*. The conjugation efficiency of pSH352p3 was $(6.5 \pm 1.8) \times 10^{-7}$, pSH500p2 was $(1.5 \pm 0.2) \times 10^{-6}$, pSH552p2 was $(3.6 \pm 0.6) \times 10^{-7}$ (Table S4).

G. mellonella infection model

Six isolates with different virulence scores were chosen to conduct the *G. mellonella larvae* infection experiment (Fig S2). After 18 h of injection, the hypervirulent NTUH-K2044 strain showed 100% mortality, slightly higher than in larvae injected with SH352 and SH416 ($P = 0.0446$). The group SH419, SH503, SH509, and SH552 achieved 100% mortality at 18 h, 72 h, 18 h, 48 h, and 48 h, respectively. There was no statistical difference between the other groups. These results indicated that SH352 and SH416 had lower virulence than the NTUH-K2044 strain, and strains with higher virulence scores were about as virulent as NTUH-K2044.

Discussion

Hv-CRKP is currently documented in many countries and regions across the globe, causing more mortality than CRKP strains.[28] Here, we described the genomic characteristics and epidemiology of Hv-CRKP strains in this Jinshan hospital.

Our results indicated that Hv-CRKP is becoming an increasingly relevant clinical infectious agent in this hospital. The proportion of ICU patients with Hv-CRKP was substantially higher than that in other departments. We hypothesize that ICU patients are at a higher risk of Hv-CRKP

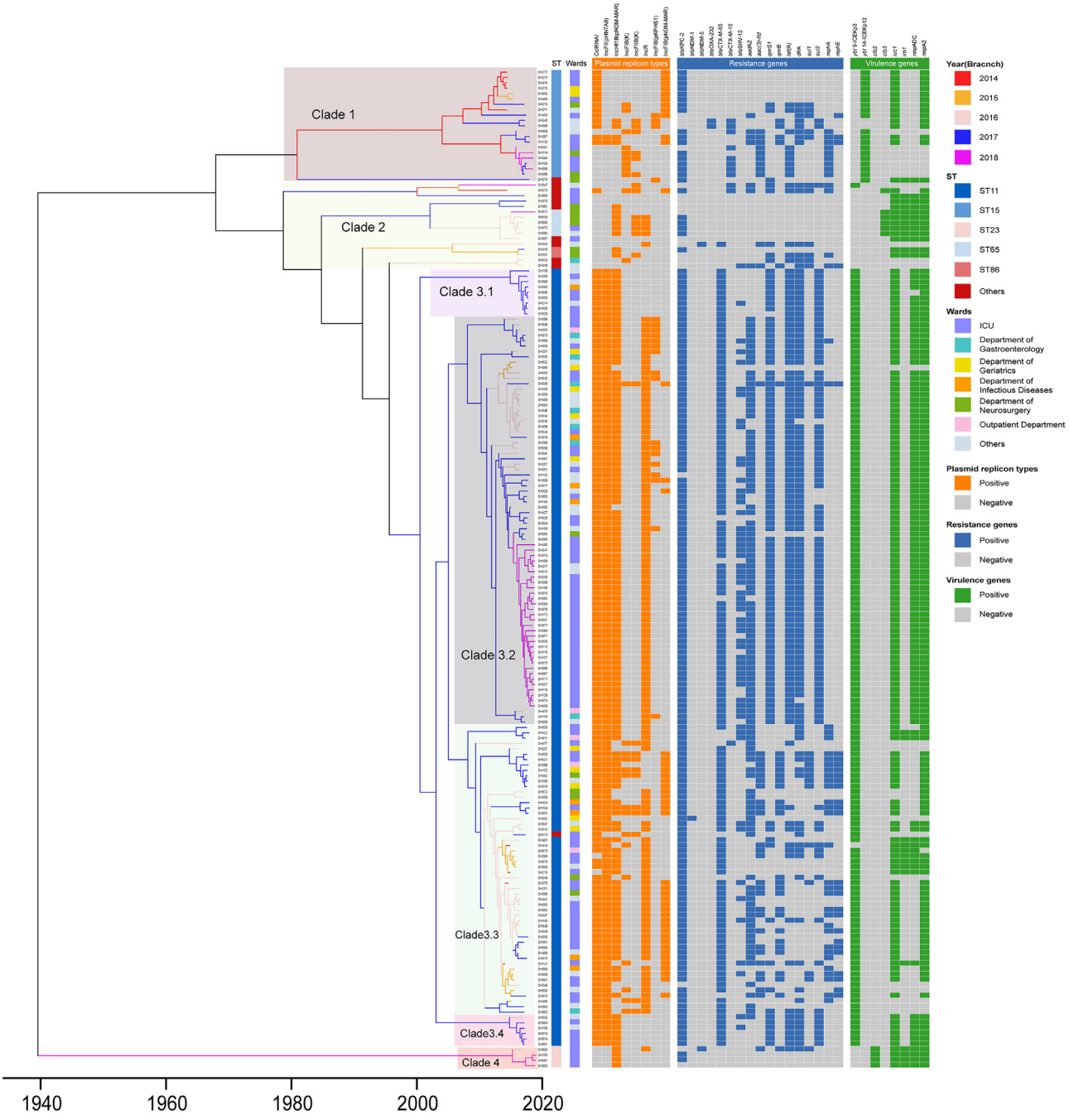

Figure 1. Timed phylogenetic tree of 186 clinical *K. pneumoniae* isolates. The branch lengths are scaled in years and are colored according to the isolation time. ST, wards, plasmid replicon types, antimicrobial resistance genes, and virulence genes present in each strain.

infections due to immune status alteration, significantly higher antimicrobial exposure than in other departments, and more invasive procedures during treatment.[29]

The Hv-CRKP strains exhibited high resistance to carbapenems, aminoglycosides, fluoroquinolones, and cephalosporins. The aminoglycoside resistance mechanism eventually moved from *aac(3)-IId* to *aadA2*. Changes in the predominance of *sul1* and *sul2* imply that sulfanilamide resistance may be mediated dominantly by *sul2*. Additionally, polymyxin resistance was identified in two isolates, which possessed *mgrB* truncation. Our data demonstrated that all Hv-CRKP strains remained susceptible to tigecycline, a higher susceptibility level than in earlier research.[29]

Seven STs were identified among 155 Hv-CRKP isolates in this hospital, indicating a higher clonal number than the non-Hv-CRKP in this hospital. Among the seven STs, ST11 increased sharply and became the most common ST. Comparative genomics also revealed that ST11 was responsible for the most significant fraction of domestic Hv-CRKP. In this hospital, ST11-KL64 and ST11-KL47 were the predominant strains.

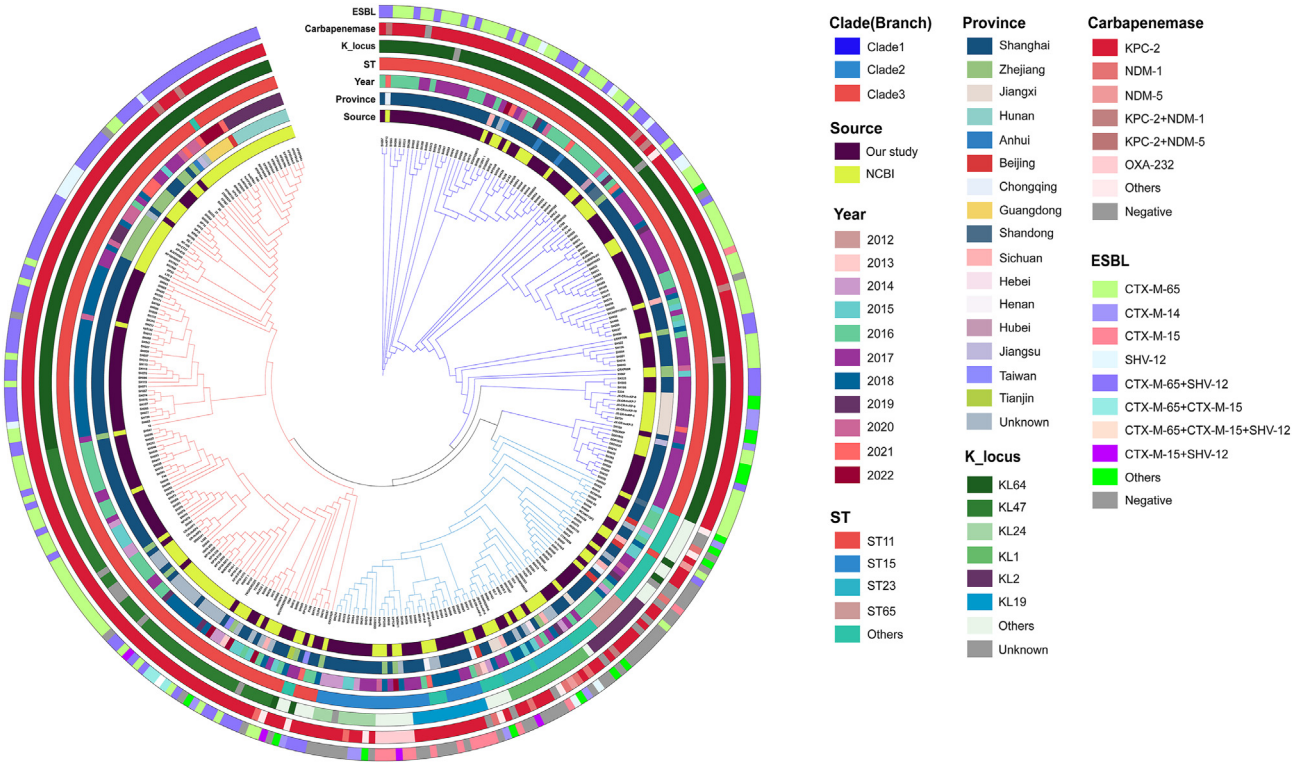

Figure 2. Phylogenetic analysis of 321 genomes of *K. pneumoniae*. Maximum likelihood phylogenetic tree constructed by core genes of 321 *K. pneumoniae* isolates. The colors of branches correspond to clades. Strips illustrated source, province, year, ST, K loci, carbapenemase, and ESBL from inside to outside.

Phylogenetic analysis of domestic *K. pneumoniae* strains revealed that clade 1 of ST11-KL64 clones and clade 3 of ST11-KL64 and ST11-KL47 clones were independent. A recent study also indicated that the ST11 clone in China was connected with KL64 and KL47.[30] It suggests that the spread of ST11-specific sublineages drives the spread of Hv-CRKP in China, underscoring the significance of genetic monitoring to detect high-risk clones during their initial propagation.

The time-based Bayesian phylogenetic tree revealed that clinical strains were separated into four clades, with Clade 3 predominant. Importantly, all inferred each Clade's most recent common ancestor predating the initial bacterial isolation. This revealed that Hv-CRKP circulated before this study. The fact that strains recovered from multiple wards within the same Clade means that nosocomial transmission occurred in this hospital. Furthermore, Hv-CRKP strains involved more wards than non-Hv-CRKP, suggesting the urgent need for stricter surveillance and infection-control measures to prevent further dissemination in nosocomial settings.[31]

It was found that bla_{KPC-2} was the most frequently identified carbapenemase gene in Hv-CRKP from 2014 to 2018. In this investigation, we found the bla_{KPC-2} gene on the IncFII and FII (pBK30683) plasmids critical for horizontal gene transfer of the bla_{KPC-2} gene.[32—34] The transmission ward range and the conjugation efficiency of pSH552p2 were relatively lower than pSH500p2, indicating that the cointegrated FII plasmid has a lower transmissibility or high adaptation cost. Besides, other published plasmids p205880-NDM separated from Chongqing in 2012, pF726925-1 from Jiangsu in 2015, p628-KPC from Beijing in 2015,[35] pKPC2_020,002 from Sichuan in 2016, pJX5-2 and pJX6-2 from Jiangxi in 2018.[36] The fact that these plasmids were recovered from multiple regions in China suggests that bla_{NDM-1}-carrying pSH352p3 and bla_{KPC-2}-carrying pSH500p2 and pSH552p2 plasmids were present existed and possibly disseminated in China previously.

In addition to resistance genes, our results revealed abundant virulence genes. In this study, *iuc* was the most frequent virulence-associated gene, followed by *ybt*. *ybt9* in ICEKp3 and *ybt14* in ICEKp12 were respectively connected with ST11 and ST15 clones. This result shows that distinct clones of CRKP acquire a virulence plasmid to transform into Hv-CRKP. Furthermore, ST23 clones were highly correlated with *clb2*, whereas ST65 and ST86 clones were associated with *clb3*. The results of our infection model with *G. mellonella* demonstrated that strains with higher virulence scores have the same hypervirulent phenotype as NTUH-K2044. This study suggests that hvKP could be detected rapidly and accurately by deploying genomic techniques.

In conclusion, this study uncovered the genetic epidemiology of Hv-CRKP in Jinshan Hospital. A high degree of gene commonality was detected among the Hv-CRKP in this hospital, specifically the ST11-KL64 and ST11-KL47 clones, prone to horizontal spreading throughout hospital wards. Therefore, there is an immediate need to increase surveillance for Hv-CRKP, deploy molecular and genomic technologies for accurate and quick detection of high-risk

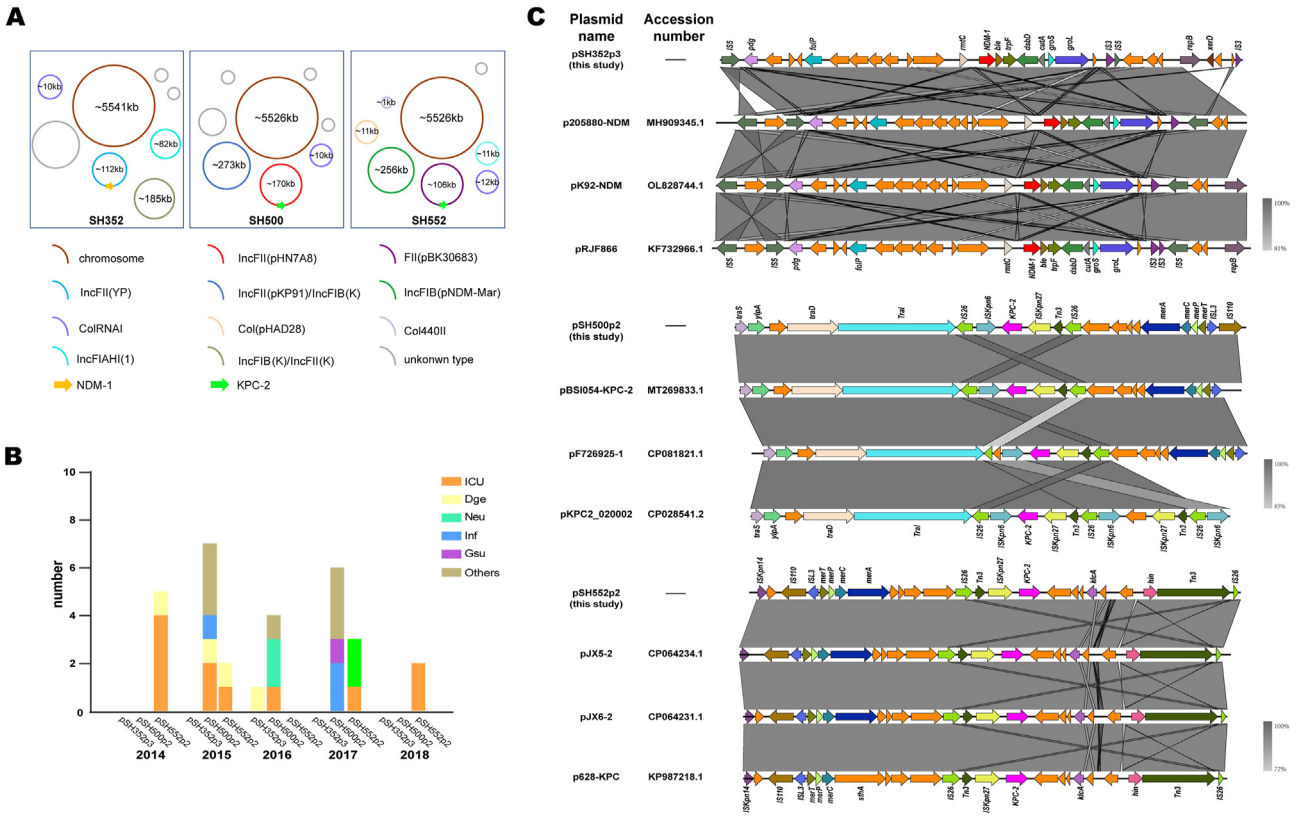

Figure 3. Characteristics of bla_{KPC-2} carrying and bla_{NDM-1} plasmids. (A). The circular genetic map of the three *K. pneumoniae* strains plasmids harboring the KPC-2 and NDM-1 genes. (B). Distribution of pSH500p2, pSH552p3, and pSH352p3 inwards between 2014 and 2018. Abbreviations: ICU, intensive care unit; Dge, department of geriatrics; Neu, Department of Neurosurgery; Inf, Department of Infectious Diseases; Gsu, Department of Gastroenterology. (C). Genetic environment of bla_{KPC-2} and bla_{NDM-1} genes in the plasmids. pSH352p3 was compared with the reference plasmids p205880-NDM, pK92-NDM, and pRJF866. pSH500p2 was compared with the reference plasmids pBSI054-KPC2, pF726925-1, and pKPC2_020,002. pSH552p3 was compared with the reference plasmids pJX5-2, pJX6-2, and p628-KPC. Arrows show the positions and directions of the genes: red arrows, NDM-1; pink arrows, KPC-2; orange arrows, CDS; other colored arrows, transposase and integrase. Regions exhibiting sequence homology are shown in gray.

Hv-CRKP clones, and take stringent measures to control its further spread in this institution.

Funding source

This study was supported by the National Key Research and Development Program of China (No. 2018YFC1603900).

Ethical approval statement

The protocol for this study was approved by the Ethics Committee of Shanghai Public Health Clinical Center (No. 2017-S027-08). Due to the retrospective nature of the study, the need for approval was waived by the Ethics Committee of Shanghai Public Health Clinical Center, and all the patient data enrolled in this study were anonymized.

Conflicts of interest

All authors disclosed no relevant relationships.

References

1. Meatherall BL, Gregson D, Ross T, Pitout JD, Laupland KB. Incidence, risk factors, and outcomes of Klebsiella pneumoniae bacteremia. *Am J Med* 2009;**122**:866–73.
2. Navon-Venezia S, Kondratyeva K, Carattoli A. Klebsiella pneumoniae: a major worldwide source and shuttle for antibiotic resistance. *FEMS Microbiol Rev* 2017;**41**:252–75.
3. Russo TA, Marr CM. Hypervirulent Klebsiella pneumoniae. *Clin Microbiol Rev* 2019;**32**.
4. Alcántar-Curiel MD, Girón JA. Klebsiella pneumoniae and the pyogenic liver abscess: implications and association of the presence of rpmA genes and expression of hypermucoviscosity. *Virulence* 2015;**6**:407–9.
5. Agyeman AA, Bergen PJ, Rao GG, Nation RL, Landersdorfer CB. A systematic review and meta-analysis of treatment outcomes following antibiotic therapy among patients with carbapenem-resistant Klebsiella pneumoniae infections. *Int J Antimicrob Agents* 2020;**55**:105833.
6. Zhang R, Zhou HW, Cai JC, Chen GX. Plasmid-mediated carbapenem-hydrolysing beta-lactamase KPC-2 in carbapenem-resistant Serratia marcescens isolates from Hangzhou, China. *J Antimicrob Chemother* 2007;**59**:574–6.

7. Tian D, Wang M, Zhou Y, Hu D, Ou HY, Jiang X. Genetic diversity and evolution of the virulence plasmids encoding aerobactin and salmochelin in Klebsiella pneumoniae. *Virulence* 2021;**12**:1323—33.
8. Zhang Y, Jin L, Ouyang P, Wang Q, Wang R, Wang J, et al. Evolution of hypervirulence in carbapenem-resistant Klebsiella pneumoniae in China: a multicentre, molecular epidemiological analysis. *J Antimicrob Chemother* 2020;**75**:327—36.
9. Marr CM, Russo TA. Hypervirulent Klebsiella pneumoniae: a new public health threat. *Expert Rev Anti Infect Ther* 2019;**17**:71—3.
10. CLSI. *The performance stands for antimicrobial susceptibility testing, 30th ed CLSI supplement M100*. Clinical and laboratory standards institute; 2020.
11. Prokesch BC, TeKippe M, Kim J, Raj P, TeKippe EM, Greenberg DE. Primary osteomyelitis caused by hypervirulent Klebsiella pneumoniae. *Lancet Infect Dis* 2016;**16**:e190—5.
12. Eucast. *Breakpoint tables for interpretation of MICs and zone diameters*. The European Committee on Antimicrobial Susceptibility Testing; 2020. *Version* 10.0.
13. Chen S, Zhou Y, Chen Y, Gu J. fastp: an ultra-fast all-in-one FASTQ preprocessor. *Bioinformatics* 2018;**34**:i884—90.
14. Bankevich A, Nurk S, Antipov D, Gurevich AA, Dvorkin M, Kulikov AS, et al. SPAdes: a new genome assembly algorithm and its applications to single-cell sequencing. *J Comput Biol* 2012;**19**:455—77.
15. Seemann T. Prokka: rapid prokaryotic genome annotation. *Bioinformatics* 2014;**30**:2068—9.
16. Lam MMC, Wick RR, Watts SC, Cerdeira LT, Wyres KL, Holt KE. A genomic surveillance framework and genotyping tool for Klebsiella pneumoniae and its related species complex. *Nat Commun* 2021;**12**:4188.
17. Liu H, Xin B, Zheng J, Zhong H, Yu Y, Donghai P, et al. *Build a bioinformatic analysis platform and apply it to routine analysis of microbial genomics and comparative genomics*. 2021.
18. Didelot X, Croucher NJ, Bentley SD, Harris SR, Wilson DJ. Bayesian inference of ancestral dates on bacterial phylogenetic trees. *Nucleic Acids Res* 2018;**46**:e134.
19. Price MN, Dehal PS, Arkin AP. FastTree 2–approximately maximum-likelihood trees for large alignments. *PLoS One* 2010;**5**:e9490.
20. Letunic I, Bork P. Interactive Tree of Life (iTOL) v5: an online tool for phylogenetic tree display and annotation. *Nucleic Acids Res* 2021;**49**:W293—6.
21. Carattoli A, Hasman H. PlasmidFinder and in silico pMLST: identification and typing of plasmid replicons in whole-genome sequencing (WGS). *Methods Mol Biol* 2020;**2075**:285—94.
22. Florensa AF, Kaas RS, Clausen P, Aytan-Aktug D, Aarestrup FM. ResFinder - an open online resource for identification of antimicrobial resistance genes in next-generation sequencing data and prediction of phenotypes from genotypes. *Microb Genom* 2022;**8**.
23. Sullivan MJ, Petty NK, Beatson SA. Easyfig: a genome comparison visualizer. *Bioinformatics* 2011;**27**:1009—10.
24. Li M, Zhang H, Zhang W, Cao Y, Sun B, Jiang Q, et al. One global disseminated 193 kb high-risk hybrid plasmid harboring tet(X4), mcr or bla(NDM) threatening public health. *Sci Total Environ* 2023;**876**:162807.
25. C-Nma Partners. Database resources of the national genomics data center, China national center for bioinformation in 2022. *Nucleic Acids Res* 2022;**50**:D27—38.
26. Chen M, Ma Y, Wu S, Zheng X, Kang H, Sang J, et al. Genome Warehouse: a public repository housing genome-scale data. *Dev Reprod Biol* 2021;**19**:584—9.
27. Chen L, Chavda KD, Melano RG, Hong T, Rojtman AD, Jacobs MR, et al. Molecular survey of the dissemination of two blaKPC-harboring IncFIA plasmids in New Jersey and New York hospitals. *Antimicrob Agents Chemother* 2014;**58**:2289—94.
28. Wyres KL, Nguyen TNT, Lam MMC, Judd LM, van Vinh Chau N, Dance DAB, et al. Genomic surveillance for hypervirulence and multi-drug resistance in invasive Klebsiella pneumoniae from South and Southeast Asia. *Genome Med* 2020;**12**:11.
29. Zhang Y, Wang Q, Yin Y, Chen H, Jin L, Gu B, et al. Epidemiology of carbapenem-resistant enterobacteriaceae infections: report from the China CRE Network. *Antimicrob Agents Chemother* 2018;**62**.
30. Chen T, Wang Y, Zhou Y, Zhou W, Chi X, Shen P, et al. Recombination drives evolution of carbapenem-resistant Klebsiella pneumoniae sequence type 11 KL47 to KL64 in China. *Microbiol Spectr* 2023:e0110722.
31. Zhou Y, Wu C, Wang B, Xu Y, Zhao H, Guo Y, et al. Characterization difference of typical KL1, KL2 and ST11-KL64 hypervirulent and carbapenem-resistant Klebsiella pneumoniae. *Drug Resist Updates* 2023;**67**:100918.
32. Andrade LN, Curiao T, Ferreira JC, Longo JM, Clímaco EC, Martinez R, et al. Dissemination of blaKPC-2 by the spread of Klebsiella pneumoniae clonal complex 258 clones (ST258, ST11, ST437) and plasmids (IncFII, IncN, IncL/M) among Enterobacteriaceae species in Brazil. *Antimicrob Agents Chemother* 2011;**55**:3579—83.
33. Shi L, Feng J, Zhan Z, Zhao Y, Zhou H, Mao H, et al. Comparative analysis of bla (KPC-2)- and rmtB-carrying IncFII-family pKPC-LK30/pHN7A8 hybrid plasmids from Klebsiella pneumoniae CG258 strains disseminated among multiple Chinese hospitals. *Infect Drug Resist* 2018;**11**:1783—93.
34. Yang X, Dong N, Chan EW, Zhang R, Chen S. Carbapenem resistance-encoding and virulence-encoding conjugative plasmids in Klebsiella pneumoniae. *Trends Microbiol* 2021;**29**:65—83.
35. Wang L, Fang H, Feng J, Yin Z, Xie X, Zhu X, et al. Complete sequences of KPC-2-encoding plasmid p628-KPC and CTX-M-55-encoding p628-CTXM coexisted in Klebsiella pneumoniae. *Front Microbiol* 2015;**6**:838.
36. Huang QS, Liao W, Xiong Z, Li D, Du FL, Xiang TX, et al. Prevalence of the NTE(KPC)-I on IncF plasmids among hypervirulent Klebsiella pneumoniae isolates in Jiangxi province, south China. *Front Microbiol* 2021;**12**:622280.

Appendix A. Supplementary data

Supplementary data to this article can be found online at https://doi.org/10.1016/j.jmii.2023.10.012.